BMC Oral Health

RESEARCH

Open Access

A comparative study of the epithelial regeneration capacities of two biomaterials in vitro

Zhiwei Tian[1], Zhongqi Zhao[1], Marco Aoqi Rausch[1,2], Christian Behm[1], Dino Tur[3], Hassan Ali Shokoohi-Tabrizi[4], Oleh Andrukhov[1*] and Xiaohui Rausch-Fan[3,5]

Abstract

Background Regeneration of periodontal epithelium remains a major focus in current dental research, with various exogenous substitute materials being applied in clinical practice. Yet, the highly organized structure of native tissue still poses considerable challenges for biomaterials attempting to mimic the original environment. In this study, we investigated the effects of a newly developed gelatin/polycaprolactone nanofiber (GPF) and a micro-scaled collagen matrix (CM) on the biological behavior of oral epithelial Ca9-22 cells, aiming to assess the clinical applicability of the materials and conducted a preliminary exploration of the interplay between the Ca9-22 cells and the material properties.

Methods The oral epithelial Ca9-22 cell line was cultured onto the GPF, CM, and tissue culture plate (TCP) for 3, 7, and 14 days. Cell morphology, attachment proliferation/viability, the gene expression of keratin 14 (KRT14), keratin 10 (KRT10), integrin β-1 (ITGB-1), intercellular adhesion molecule 1 (ICAM-1), interleukin 8 (IL-8) and interleukin 1β (IL-1β), the levels of IL-8 proteins were evaluated.

Results Ca9-22 cells exhibited distinct adhesion morphology and distribution patterns on two biomaterials. After 3 days of culturing on GPF, Ca9-22 cells demonstrated higher levels of proliferation/viability compared to those on CM. In most situations, except KRT10, both materials effectively stimulated gene and protein expression related to epithelial regeneration and wound healing, especially in the early stage of culture. Compared to CM, GPF demonstrated a stronger stimulation of KRT14 expression at day 3 and a more significant enhancement of KRT10 expression after 7 and 14 days. However, it was less effective at promoting IL-8 expression after 3 days than the former. The gene expression of KRT10 was suppressed by CM at day 7. The IL-8 protein production was the highest in cells grown on CM.

Conclusion The morphology and cellular functions of oral epithelial cells differed between GPF and CM. Both materials are capable of promoting epithelial regeneration; however, GPF is more conducive to functional stratification of newly formed epithelium, while CM holds a more sustained effect on epithelial proliferation.

Keywords Polycaprolactone, Gelatin, Nanofiber, Collagen, Epithelial regeneration, Biomaterials

*Correspondence:
Oleh Andrukhov
oleh.andrukhov@meduniwien.ac.at

Full list of author information is available at the end of the article

Introduction

The periodontium is a considerably structurally intricate and complex unit, mainly consisting of gingiva, periodontal ligament, cementum and alveolar bone from a histological perspective. The oral epithelium acts as the first line of protection between the underlying periodontal tissues and the external milieu [1]. The epithelial tissue engages in the immune and inflammatory responses to exogenous antigens by producing a range of relevant cytokines and chemokines [2]. Once this structure is breached, it can lead to numerous periodontal and mucosal diseases, with periodontitis being the most common [3, 4]. Hence, whether in prophylaxis or treating existing conditions, ensuring the integrity of the epithelial barrier in periodontium is a top priority [5].

From the cellular level, during the epithelial regeneration process, oral epithelial cells reestablish the stratified structure of the epithelium through proliferation, migration and differentiation [6]. These biological events are regulated by various proteins, particularly keratins 10 and 14 (KRT10 and KRT14), integrin β-1 (ITGB-1), and intercellular adhesion molecule 1 (ICAM-1) [7–9]. By releasing chemokines and cytokines, such as interleukin 8 (IL-8) and interleukin 1β (IL-1β), they promote the recruitment of inflammatory cells and facilitate the elimination of pathogens and cell debris [6, 10, 11]. Consequently, effectively inducing and leveraging the proper biological functions of oral epithelial cells has always been in focus for periodontal tissue repair and regeneration [12].

The goal of tissue engineering involves employing different scaffold materials to provide a suitable extracellular environment for specific cell types, effectively inducing cell behavior to ultimately facilitate the regeneration of target tissues [13]. Due to the diversity of their components and characteristics, polymers can be effortlessly molded into more complex physical and chemical constructs, and their biodegradable property makes them extensively employed as bioscaffolds [14]. Among numerous natural polymers, collagen, as one of the major protein elements of the extracellular matrix (ECM), is commonly used in tissue engineering for its superb biocompatibility. In recent years, a new type of collagen-based matrix (CM), which is chemically crosslinked to enhance its mechanical properties, has been shown to be effective for regenerating periodontal soft tissues in both in vitro and in vivo studies [15, 16].

Gelatin, another natural polymer derived from the hydrolysis of collagen, exhibits favorable biophysical and biochemical properties, making it widely applicable in the fields of medicine and tissue engineering [17, 18]. Furthermore, previous research has shown that electrospinning gelatin fibers can support the adhesion and proliferation of oral keratinocytes [19]. Natural polymers commonly suffer from inferior mechanical properties and to overcome these limitations, the combination of different natural or synthetic polymers with desirable physicochemical traits was proposed [20]. Polycaprolactone (PCL) is a synthetic polymer with notable mechanical properties and a proper degradation rate in the body, making it an ideal choice for composite materials [21]. Recently, a prototype of a nanometer-scale gelatin/PCL fiber (GPF) fabricated via electrospinning has been developed. In our recent study, the GPF promoted the biological function of gingival mesenchymal stromal cells in vitro, suggesting it may positively contribute to the angiogenesis and the regeneration of gingival connective tissue [22]. However, it remains uncertain whether this structure benefits the functional regeneration of oral stratified epithelium.

Our current study aims to explore the effects of the GPF on the biological behaviors of oral epithelial cells, comparing these findings with the clinically applied CM to evaluate the feasibility of GPF for clinical use in reconstructing keratinized epithelial tissue.

Materials and methods

Creation of experimental sample for GPF and CM

To obtain material samples suitable for the size of a cell culture well plate, GPF specimens with fibers approximately 550 nm in diameter and an elastic modulus near 3 kPa (Neo Modulus [Suzhou] Medical, Suzhou, China) measuring 6 mm in diameter were prepared using a disinfected corneal trephine (Shimei Medical, Shenzhen, China). Simultaneously, CM (Fibro-Gide®, Geistlich Pharma AG, Wolhusen, Switzerland) was trimmed to 3 mm thickness, from which 6 mm circular samples were punched out. The further detailed original structure of materials can be found in the previous study [23]. All the specimens were subsequently placed at the bottom of 96-well plates for further investigation.

Cell culture

In this study, we selected the human oral squamous carcinoma Ca9-22 cell line (Japanese Collection of Research Bioresources Cell Bank, JCRB0625, Ibaraki, Japan) as our experimental model. This cell line reflects most properties of primary oral epithelial cells while overcoming their rapid cell senescence, making it ideal for long-term studies [24–26]. Ca9-22 cells were cultured in modified Eagle's minimum essential medium (MEM, Gibco®, Carlsbad, CA, USA), supplemented with 10% fetal bovine serum (FBS, Gibco, Carlsbad, USA), 100 U/ml penicillin and 50 μg/ml streptomycin (P/S, Gibco, Carlsbad, CA, USA). Cells were maintained at 37 °C in a controlled environment containing 5% CO_2 and 95% humidity and used in the experiments in passages from the fourth to sixth.

Scanning electron microscopy and fluorescence microscopy

Cell morphology was first analyzed using scanning electron microscopy (SEM) [27]. Ca9-22 cells were cultured onto GPF and CM scaffolds at a seeding density of 5×10^3/well in 200 µL of MEM and incubated at 37℃. Following 3, 7 and 14 days, the samples were fixed with 4% paraformaldehyde (ThermoFisher Scientific, Waltham, USA). Subsequently, all materials with cells underwent a series of ethanol dehydration gradients before drying with hexamethyldisilazane (HMDS, Sigma-Aldrich, St. Louis, USA). Finally, the samples were sputter-coated and analyzed using an SEM (FEI Quanta 200, Hillsboro, OR, USA) at 15 kV accelerating voltage.

To further evaluate the morphological differences between cells adhered to distinct structures, actin cytoskeleton and nuclei were visualized by fluorescence microscopy. Cells were seeded similarly as in SEM experiments and fixed using 4% paraformaldehyde (ThermoFisher Scientific, Waltham, USA) for 15 min at room temperature after 3, 7 and 14 days. The samples were then permeabilized with 0.1% Triton-X100 for 5 min. Following a blocking step of 30 min with 1% bovine serum albumin, they were stained with rhodamine-conjugated phalloidin (1:200 in PBS, ThermoFisher Scientific, Waltham, USA) and 4′, 6-diamidino-2-phenylindole (DAPI, 1:1000 in PBS, Sigma-Aldrich, St. Louis, MO, USA) to visualize actin cytoskeleton and nuclei, respectively. Stained cells were visualized using an ECHO Revolve fluorescence microscope (Echo, San Diego, CA, USA).

Cell proliferation/viability

Cell Bank, 5×10^3 of Ca9-22 cells were seeded onto the surfaces of GPF, CM and TCP in 200 µl of MEM, and the proliferation/viability of the cells was determined using a cell counting kit (CCK-8, Dojindo Laboratories, Japan) after 3, 7, and 14 days as previously described [22]. Twenty microliters of CCK-8 reagent was added to each sample, and after 4 h of incubation, the optical density values were measured at a wavelength of 450 nm using a microplate reader (Synergy HTX; BioTek).

RT-qPCR

Ca9-22 cells were seeded on three different materials at a density of 3×10^4/well in 200 µl of medium. After 3, 7 and 14 days, the cells were lysed, and the lysates were transcribed into cDNA using "Cells-to-CT Lysis Reagents" and "RT reagents" (both Invitrogen, Carlsbad, CA, USA), The reverse transcription reaction was performed at 37 °C for 1 h, then the temperature was raised to 95 °C for 5 min using the Primus 96 advanced thermocycler (Peq/Lab/VWR, Darmstadt, Germany) [28]. RT-qPCR was performed using the following TaqMan gene expression assays (Applied Biosystems, Foster City, USA): KRT10 (Hs00166289_m1), KRT14 (Hs00265033_m1), ITGB-1 (Hs01127536_m1), ICAM-1 (Hs00164932_m1), IL-1β (Hs01555410_m1), IL-8 (Hs00174103_m1) at following conditions: 10 min of initial heating at 95 °C followed by 50 cycles at 95 °C for 15 s and at 60 °C for 1 min using a QuantStudio 3 device (Applied Biosystems, Foster City, USA). Target gene expression levels were calculated by the $2^{-\Delta\Delta Ct}$ method, employing GAPDH as the housekeeping gene and the results from the 3-day TCP group as the reference control; the relative fold changes in gene expression level for each group at different time points were calculated based on these results. This was done to better visualize the time course of changes in gene expression across all groups. The calculation formula was as follows: $\Delta\Delta Ct = (Ct^{target} - Ct^{GAPDH})_{sample} - (Ct^{target} - Ct^{GAPDH})_{control}$.

ELISA

The level of IL-8 protein in the conditioned medium was determined after 3, 7 and 14 days of incubation using a human IL-8 ELISA kit (Cat. Nr. 88-8086, ThermoFisher Scientific, Waltham, USA) according to the guidelines of the manufacturer. The quantitative analysis was conducted using the Synergy HTX multi-mode reader (BioTek Instruments, Winooski, USA).

Statistical analysis

Each experiment was repeated 5 times, and all quantitative data are presented as mean ± standard deviation (SD) of these 5 independent repetitions. Relevant data analysis was performed using GraphPad Prism software (version 9, La Jolla, CA, USA). The normality of distribution was confirmed by the Kolmogorov-Smirnov test and one-way ANOVA for repeated measures followed by a post-hoc LSD test was applied to determine differences among groups. The nonparametric Friedman test was used for data that did not follow the normal distribution. A p-value < 0.05 was considered statistically significantly different.

Results

Cell attachment and morphology

The attachment of Ca9-22 cells on different scaffolds, along with their intrinsic structural features, was first analyzed using SEM (Fig. 1). The fibers of GPF were randomly oriented with fairly uniform diameters, whereas fibers in CM structure exhibited a sheet-like configuration with larger pore sizes between the fibers. Cells attached and grew on the GPF, showing typical cobblestone and oval-shaped morphologies after 3 days of culture. Some cells even migrated under the nanofibers, intertwining with the GPF structures. The cells further bonded tightly to their neighboring cells, gradually forming small cell sheets. Over the 2 weeks of culture, the

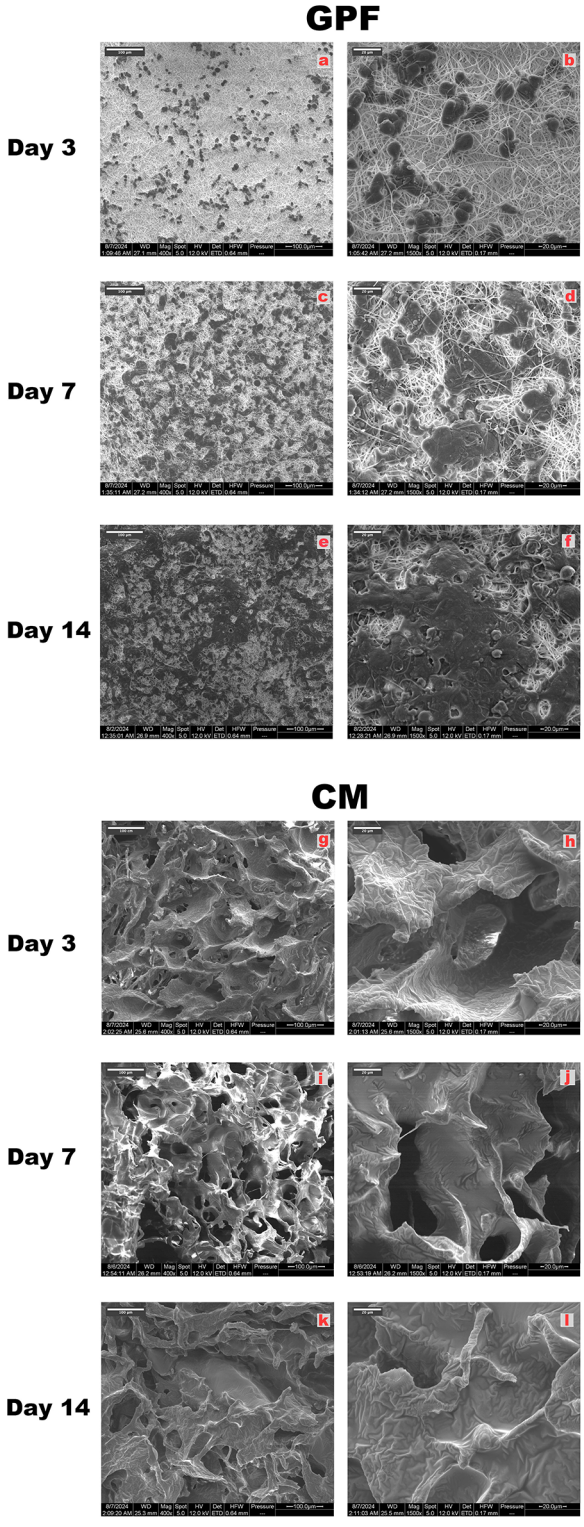

Fig. 1 Observation of cell adhesion and growth on two scaffolds using SEM. Representative SEM images of Ca9-22 cells cultured on GPF (**a**-**f**) and CM (**g**-**l**). Cells were incubated for 3 days (**a**, **b**, **g**, **h**), 7 days (**c**, **d**, **i**, **j**), and 14 days (**e**, **f**, **k**, **l**), with images taken at 400× (**a**, **c**, **e**, **g**, **i**, **k**) and 1500× (**b**, **d**, **f**, **h**, **j**, **l**) magnification. Scale bars represent 20 µm and 100 µm, respectively. Over time, cells cultured on GPF formed interconnected sheet-like structures that covered most of the scaffold's surface fibers

number of cells steadily increased, eventually covering most of the surface of the materials. However, it was difficult to discriminate cells' adhesion to CM. This could be due to the similarity between the cellular structure and the surface texture of materials. Furthermore, the pore size of CM is large enough to enable cell migration inside this scaffold.

Subsequently, the actin cytoskeleton and cell nuclei were visualized by specific staining to further evaluate the morphology of Ca9-22 cells on different substrates and compare them to tissue culture plastic (Fig. 2). On the 3rd day of culture, numerous cells in contact with their neighbors and forming cluster-like structures was observed in cells growing on GPF. However, the intensity of spreading cells was slightly lower than that of TCP. Contrastingly, the CM group displayed few cells with oval-shaped morphology sparsely distributed on the material. During the experiments, an increased number of cells was observed for both substrates; however, the cell number was visually higher on GPF compared to CM. Furthermore, the cell number on both membranes was lower than that observed for TCP. Some differences were also observed in cell morphology: cells on GPF largely maintained the oval shape, whereas, on CM and TCP, they exhibited elongated into polygonal shapes, featuring decreased roundness and increased aspect ratios.

Cell proliferation/viability

The proliferation/viability of Ca9-22 cells seeded onto different substrates and measured by the CCK-8 method is presented in Fig. 3. In line with the microscopy observations, cells demonstrated stable and sustained proliferation on all substrates during the 2-week culture period. Among them, the TCP control group had a higher proliferation level compared with the other two groups, although this gap gradually narrowed over time. Furthermore, on day 3, the cell viability for the CM group was significantly lower than that of the GPF group, but on days 7 and 14, no differences between the two materials were observed.

Functional gene expression and IL-8 production

The expression of functional genes in Ca9-22 cells grown on different substrates after 3, 7, and 14 days of culturing is presented in Fig. 4. The expression level of KRT14 was higher in cells growing on both materials than those grown on TCP, but significant differences were observed for GPF after day 3 and for CM after day 14. The expression level of KRT10 was constantly higher in Ca9-22 cells growing on GPF than those growing on CM. The gene expression of ITGB-1 and ICAM-1 was significantly higher on both materials compared to TCP after 3 days of culture. However, at later time points, a significant difference was found only for ITGB-1 and ICAM-1 for CM

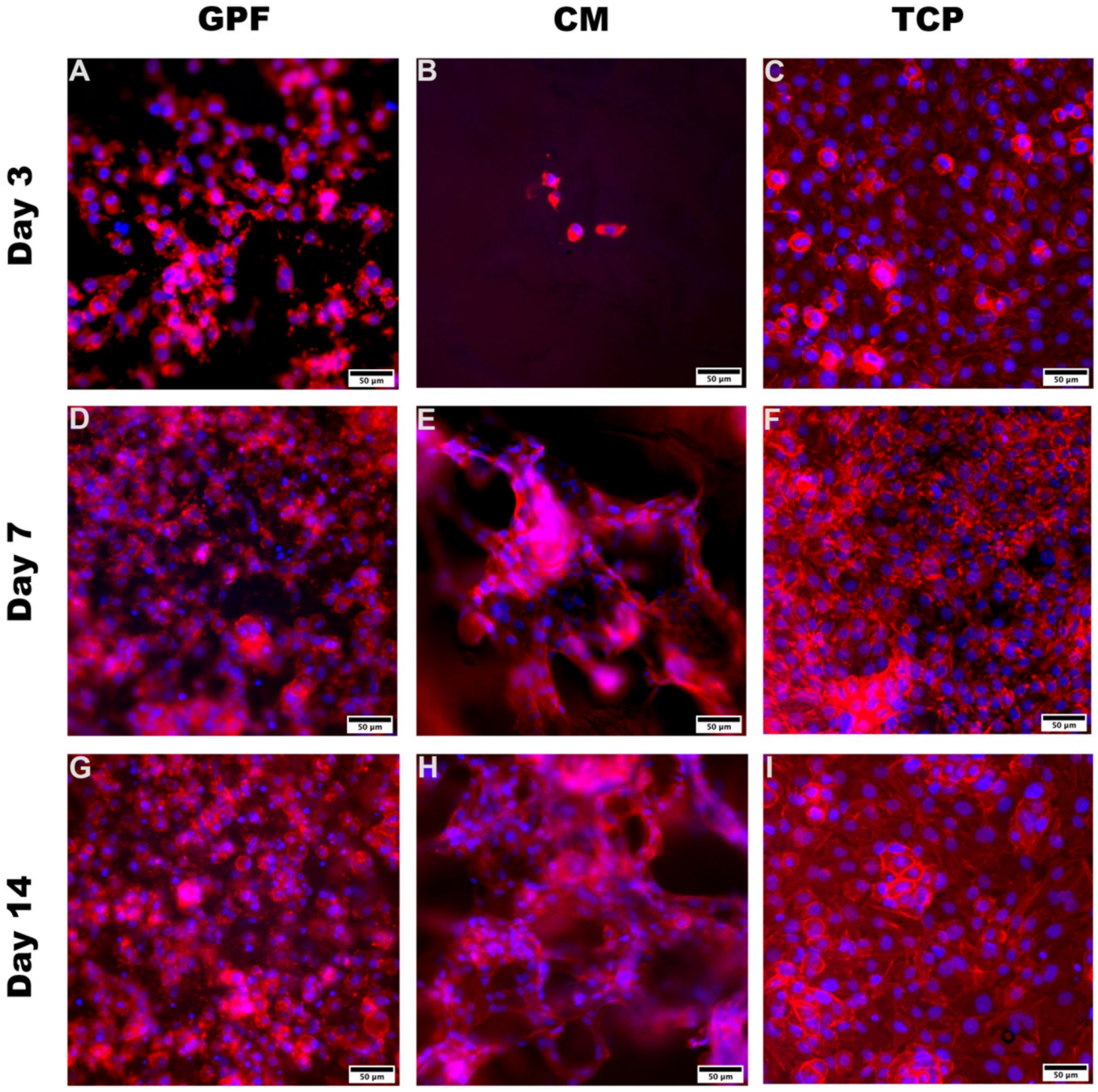

Fig. 2 The morphological characteristics and distribution pattern of oral epithelial cells on different substrates. Fluorescence microscopy images illustrating Ca9-22 cells cultured on GPF (**A**, **D**, **G**), CM (**B**, **E**, **H**), and TCP (**C**, **F**, **I**). The images highlight a representative experiment, showing actin filament staining (red) and nuclei staining (blue) after 3 (**A**-**C**), 7 (**D**-**F**), and 14 (**G**-**I**) days of culture. Images were captured at 100× magnification (10x eyepiece and a 10x objective lens), with a scale bar representing 50 µm

at day 7. No differences between GPF and CM regarding the expression of these two proteins were found. On days 3 and 7, the expression of IL-8 was significantly higher in cells growing on both materials compared to TCP. Moreover, on day 3, significantly higher IL-8 gene expression was observed for CM compared to GPF. Finally, the expression of IL-1β at days 3 and 7 was significantly higher in cells growing on GPF compared to TCP.

The content of IL-8 protein in the conditioned media is presented in Fig. 5. Cells growing on the CM membrane exhibited the highest levels of IL-8 production, which were significantly higher than those for GPF and TCP ($p < 0.05$) throughout the whole observation period. The production of IL-8 by cells growing on GPF and TCP was similar, except on day 7, at which slightly but significantly higher IL-8 levels on TCP compared to GPF were observed ($p < 0.05$).

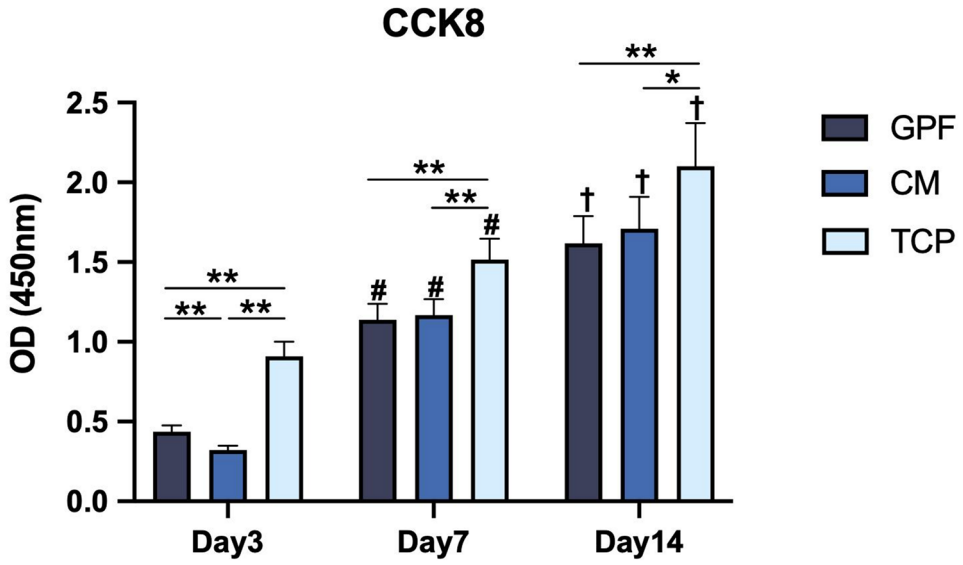

Fig. 3 Evaluation of oral epithelial cells proliferation/viability on GPF, CM and TCP. Cell proliferation/viability was assessed using CCK-8 assay after 3, 7 and 14 days; cells cultured on TCP served as control. The Y-axis shows the OD values measured at 450 nm and presented as mean ± SD of five replicates ($n = 5$). Statistical differences between each group from the same culture time are indicated by * ($p < 0.05$) and ** ($p < 0.01$). Comparisons over time for the same material, specifically between 3 and 7 days, and between 7 and 14 days, are marked with # ($p < 0.01$) and † ($p < 0.01$), respectively

Discussion

Although the question of how different scaffolds influence oral epithelial regeneration is essential, this topic remains poorly understood [29, 30]. The core principle of this approach is to minimize the potential adverse effects like excessive inflammation and immune responses and stimulate the spreading and growth of oral epithelial cells on the surface of the scaffold, which acts similarly to natural basement membranes. An ideal scaffold is expected to support the release of essential growth factors, cytokines, and ECM production, creating the microenvironment of the tissue defect that can be reconstructed, ultimately stimulating the endogenous mechanisms of epithelial regeneration [31]. Managing the intrinsic properties of the materials to regulate the microenvironment surrounding oral epithelium is a vital step to fundamentally refining the material for clinical application [8].

The attachment and proliferation of oral epithelial cells on the matrix or scaffold are indispensable for tissue morphogenesis [32]. Additionally, their further migration is necessary for wound re-epithelialization, defect repair and prevention of chronic infections [33]. Based on the SEM results, it can be seen that during the mid-to-late stage of culture, epithelial cells on GPF progressively formed continuous, sheet-like structures resembling the ECM encircling the cells, distinct from the nanofiber structure itself, echoing findings from a prior study [7]. Furthermore, the fibers of GPF are more uniform in scale compared to CM, resulting in a consistent distribution of attachment sites and pore sizes, which seems to be one of the favorable conditions for cell adhesion and migration [34].

By observing cell morphology through cytoskeleton staining, it was evident that in the first week of early culture, more cells were observed on GPF than on CM, as the density is similar to that of TCP. In a similar vein, human esophageal epithelial cells were able to adhere to and spread on PCL/Gelatin blended nanofibers scaffold, completely covering the surface of the material after 3 days of culture [35]. The absence of epithelial cells on the surface of CM could be due to the relatively large pore size, which facilitates cell migration inside this scaffold.

Coherently, differences in cytoskeletal morphology were observed among the 3 groups. It is believed that ECM-driven anchor points ultimately determine cell morphology. Corneal epithelial cells exhibited more regular morphology when attaching to smaller-sized micro-patterned substrates, which may account for the differences in the current study [36]. It is noteworthy that the formation of sheet-like cell clusters lays the groundwork for mimicking the in vivo stratified epithelial structures, and this pattern is more prevalent in smaller nanoscale GPF and TCP. This finding is supported by previous research, where Steinberg et al. cultured immortalized human gingival keratinocytes on poly(dimethylsiloxane) micropillar structures; adequate cell adhesion could not be observed when the distance between micropillars overreached 17 μm. However, a smaller gap between micropillars is correlated with an increased presence of desmosomal protein in cells, which is essential for establishing contact between keratinocytes. A similar scenario was observed in our study, the nanoscale GPF possesses finely and densely packed fibers, whereas VSCM features larger pores and a fibrous

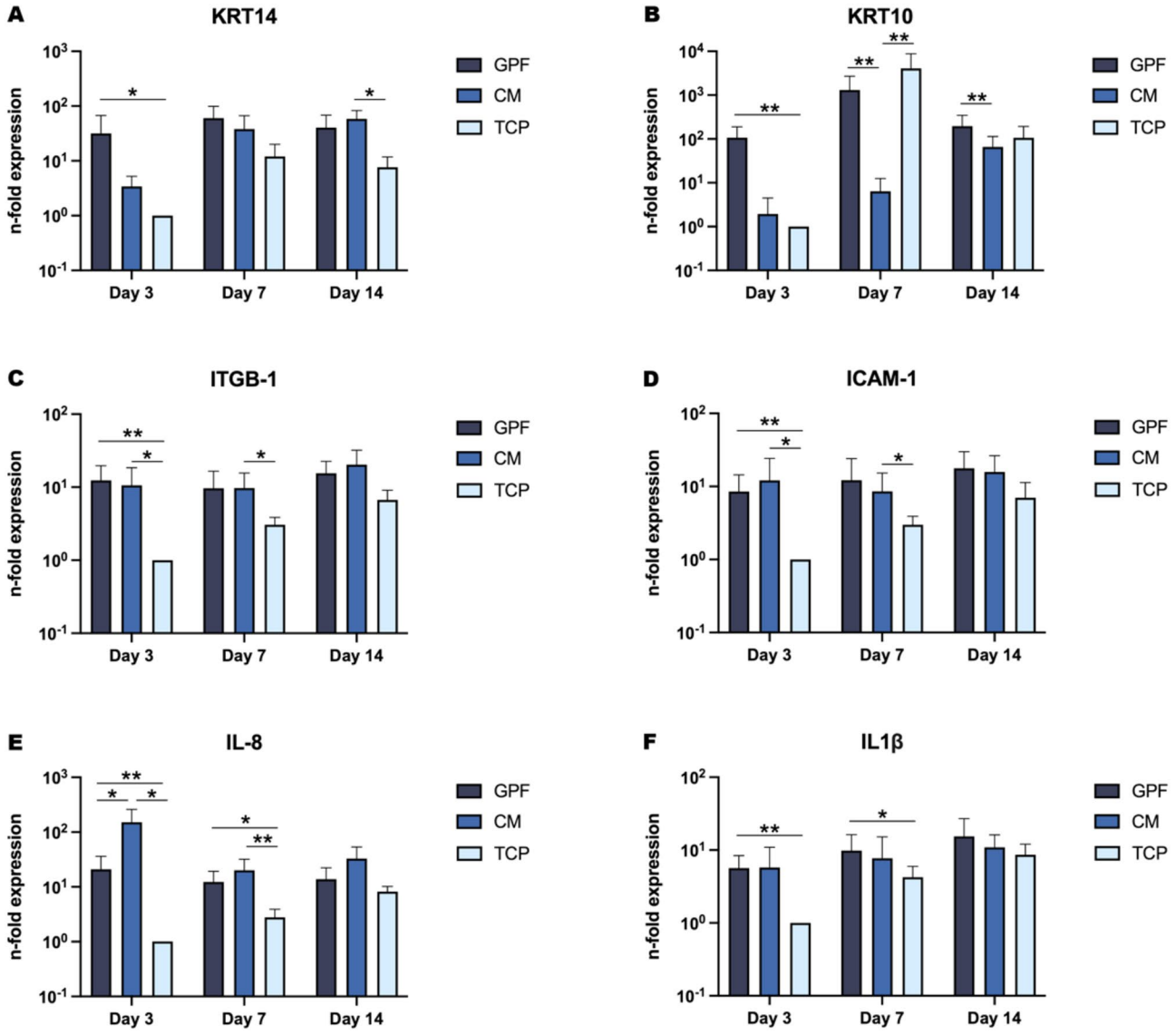

Fig. 4 Investigation of reepithelialization-related biomarkers expressed by oral epithelial cells grown on different materials. Gene expression levels of KRT14 (**A**), KRT10 (**B**), ITGB-1 (**C**), ICAM-1 (**D**), IL-8 (**E**), IL-1β (**F**) after 3, 7 and 14 days were measured by qPCR. The $2^{-\Delta\Delta Ct}$ method was used for data analysis with GAPDH as the normalization reference gene. The Y-axis illustrates the relative fold change in expression levels compared to the day-3 TCP control, where the n-fold expression is defined as 1. Results are presented as mean ± SD from five independent donors. Statistical differences between the 3 substrate groups at the same evaluation time points are denoted with * and **, indicating $p < 0.05$ and $p < 0.01$, respectively

structure, which inherently increase the challenges of initial cell adhesion and growth on the latter, resulting in the poorest adhesion outcomes [37].

As a foundation for epithelial tissue development and self-renewal, the results of proliferation/viability of Ca9-22 cells are aligned with the status of cell adhesion. Early on, the GPF group outperformed the CM group in terms of proliferation, although it consistently lagged behind the control group, with this disparity decreasing over time. The support for cell proliferation from both materials can be primarily attributed to the chemical resemblance of gelatin and collagen to the natural ECM. Nevertheless, the proliferation of different cell types is substantially impacted by their preference for the surface topography and porosity of the materials. It should be noted that the CCK-8 assay measures the metabolic activity of proliferating cells, reflecting both proliferation and viability, whereas these parameters cannot be clearly distinguished. In our experiment, the initial growth of oral epithelial cells on two materials, which differ in porosity, pore size, fiber diameter, and mechanical strength, were lower compared to TCP, which may be due to the number of adhesion sites and pore structure hindering rapid cell spreading during in vitro culture [38]. In the earlier study, Eberwein et al. suggest that smaller micropillar substrates in 5 μm are more conducive to efficient cell

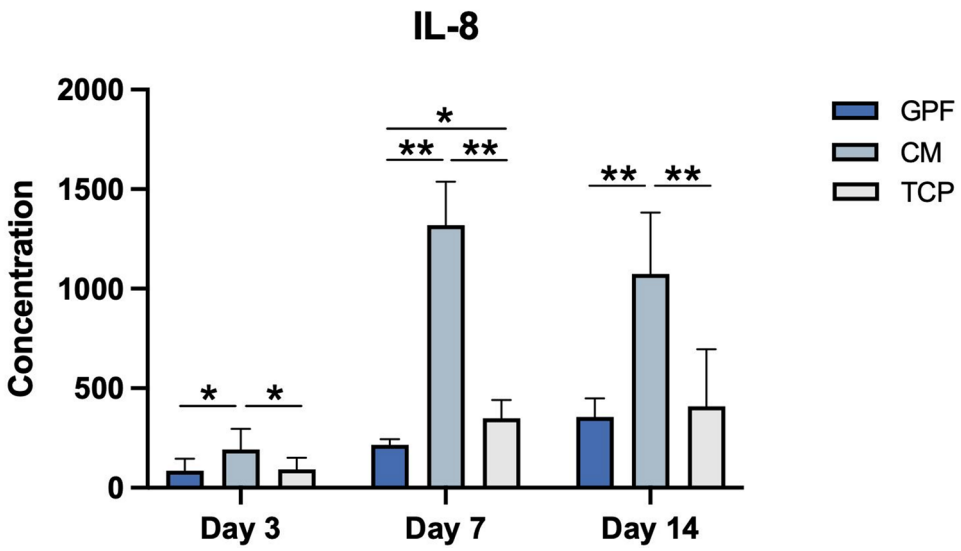

Fig. 5 Evaluation of protein production by oral epithelial cells on different substrates. IL-8 protein production by Ca9-22 cells cultured on different materials after 3, 7 and 14 days was quantitatively measured using ELISA. The Y-axis shows the IL-8 concentration in the conditioned medium, with data from 5 independent donors presented as mean ± SD. Differences between indicated groups at the same time point are indicated by * and ** for $p < 0.05$ and $p < 0.01$, respectively

proliferation and maintenance of regular cell morphology than their 11 μm counterparts, owing to differences in biomechanical patterns. The gelatin fibers on the outer layer of GPF could provide a denser array of adhesion sites, which likely contributed to the cells maintaining a regular morphology [36].

The expression of biological markers generally reflects multiple cellular functions, such as adhesion, differentiation, ECM integration and engagement in various biological cascades. These processes are the basis for achieving comprehensive tissue regeneration and maintaining dynamic physiological homeostasis in vivo [7]. Keratin is a major component of the cytoskeleton in epithelial cells, with keratin distribution in oral stratified epithelium showing specific layer-related patterns [1, 39]. In this study, GPF demonstrated a more pronounced effect compared to CM, particularly in the early stage of culture, by enhancing the expression of KRT14 and KRT10 related to epithelial regeneration and differentiation/stratification correspondingly, which parallels findings from previous studies on the role of PCL/gelatin material inducing stratified epithelial structure in vitro [7].

The integrin family, particularly ITGB-1, plays a crucial role in the adhesion of epithelial cells to the external environment, as well as in their ability to sense environmental cues and trigger signaling cascades. Additionally, ITGB-1 mediates the apical-basal polarity attachment of epithelial cells to the ECM on the basement membrane [8]. In our findings, especially in the early stage of culture, both the GPF and CM groups manifested positively modulated ITGB-1 expression. This suggests that both substrates might support the adhesion to the basement membrane.

Under physiological conditions, immune cells infiltrate the site of tissue defect and contribute to both the elimination of invading pathogens and the initiation of regenerative processes through the release of numerous biological molecules. In this context, epithelial tissue, serving as a barrier of periodontium, is critical in regulating subclinical inflammation within physiological levels and protecting against external pathogens. ICAM-1 is an essential protein mediating the infiltration of immune cells, but it also assists in the recruitment and migration of epithelial cells to the wound area and promotes the formation of healing granulation tissue, making it one of the core elements in periodontal tissue repair [9]. In this study, both materials notably enhanced the ICAM-1 level exclusively in the early stage of culture, which could be beneficial for wound healing and re-epithelialization [9, 40].

The physiological function of IL-8 is to act as a chemoattractant, enabling the migration of neutrophils to the damaged wound areas [10]. IL-8 mediates the migration and proliferation of different cell types, including epithelial cells, contributing to wound re-epithelialization [6]. In our study, we found that both materials stimulated gene expression in Ca9-22 cells. However, IL-8 protein production was higher for CM compared to GPF. Notably, the protein and gene expression levels in the GPF group did not fully correspond, which may be influenced by the physical properties and mechanical environment provided by materials acting on post-transcriptional regulation [41]. In addition, beyond possibly affecting the cell adhesion patterns, the electrostatic trait of GPF could

also have a potential absorptive effect on nearby bioactive proteins [42]. Furthermore, our recent investigation into this phenomenon revealed that GPF and CM exhibited distinct absorption and release profiles for proteins/cytokines. Both scaffolds were capable of absorbing and retaining some proteins, but qualitative and quantitative differences were observed between these materials [43], which might explain the inconsistencies between qPCR and ELISA data. GPF also enhanced the IL-1β expression during the first week, while the effect of CM was less pronounced. However, on the protein level, IL-1β was below the detection limit of ELISA. Inflammation is a double-edged sword in tissue regeneration: on the one hand, it is necessary to remove the invading microorganisms and cell debris during the inflammatory phase, and on the other hand, it might delay a healing process. We have seen that both materials stimulate the inflammatory response of Ca9-22 cells, but how much they contribute to the healing process is not known.

The surface topography and biomechanical cues of materials are garnering increasing attention in research [7]. Speaking from material-induced cell activation, both aggregation and settling of target cells and the production of subsequent growth factors and cytokines are critical for wound healing and tissue regeneration. More importantly, there is an optimal threshold for the materials' properties [36, 44]. In our study, both materials mediated cellular responses differently compared to TCP, suggesting the potential for further activation of cells in the host environment. This effect may be linked to differences in fiber size and arrangement between GPF and VSCM, which result in distinct surface topography features, determining the cellular adhesion morphology. Prior research has shown that adaptive changes in the cell cytoskeleton, triggered by the surface characteristics of a material, can lead to different cell differentiation patterns [45]. Such contact-guided adaptation might even involve rearrangements of nuclear proteins [46]. Furthermore, differences in mechanical properties could be another reason to explain the variations in cellular regulation among the 3 substrates; The internal core PCL structure in GPF substantially compensates for the low strength of the gelatin layer, potentially enhancing its adaptability in host tissue [47]. Interestingly, whether the changes from morphological or mechanical signals from the ECM suggest a link with the mediation of the integrin family, offering valuable insights for future exploration [8, 44]. Thus, although this study was conducted in vitro, it provided valuable insights and contributed positively to understanding the effect of material characteristics on cellular behavior. In this sense, it represents an indispensable part of the preclinical exploration of material performance.

However, due to the limitations of the in vitro cell culture environment, our investigation cannot truly mimic the physiological three-dimensional dynamic conditions present in the host body. The absence of fluid dynamics and extracellular biochemical signaling networks in vivo might restrict the exploration of the authentic potential of materials for clinical applications. Additionally, the comprehensive interactions and crosstalk between different cell types, as well as between cells and materials in vivo, still require further investigation. To this end, conclusions drawn solely from cellular behavior may still require further corroboration through in vivo and clinical studies. It is worth mentioning that recent animal and clinical studies have shown that VSCM effectively supported gingival soft tissue augmentation [48, 49].

Moreover, we did not use primary epithelial cells to start our test on the regenerative capacity of two materials due to the technical challenges for isolating and propagating these cells in vitro. For instance, epithelial cells might be contaminated with the fibroblast population, which may interfere with the final data accuracy [25, 50]. Additionally, primary epithelial cells generally undergo senescence rapidly, and certain cell characteristics could considerably change with increasing passages [36]. Importantly, immortalized and/or cancerous epithelial cell lines have been recognized for accurately mimicking many gingival epithelial features in vitro [36, 51]. Therefore, as an alternative, we selected the gingival-derived Ca9-22 cell line, which has been widely used in oral epithelial functional research [25, 52, 53]. This cell line possesses stable properties with minimal batch-to-batch variation, thus ensuring accurate experimental outcomes and serving as a reliable research model [54]. However, it is known that they have some differences compared to oral epithelium, especially in the expression of keratins [55]. Nevertheless, due to some inherent differences, primary epithelial cell evaluations will remain indispensable when technical limitations can be overcome in the future.

Conclusions

The current study observed that both GPF and CM supported the adhesion and proliferation of oral epithelial cells on their respective structures, each exhibiting distinct morphology and distribution of cell attachment. Both materials effectively stimulated the gene and protein expression related to epithelial regeneration and wound healing in the early stage of culture, with GPF showing a stronger positive effect on epithelial regeneration and stratification and lower

inflammatory response at the cellular level; however, given the relatively biased outcome associated with in vitro studies, further in vivo testing to confirm the validity is still necessary.

Abbreviations

GPF	Gelatin/ Polycaprolactone nanofiber
CM	Collagen matrix
TCP	Tissue culture plate
KRT14	Keratin 14
KRT10	Keratin 10
ITGB-1	Integrin β-1
ICAM-1	Intercellular adhesion molecule 1
IL-8	Interleukin 8
IL-1β	Interleukin 1β
ECM	Extracellular matrix
PCL	Polycaprolactone
SEM	Scanning electron microscopy

Acknowledgements
The authors would like to thank Phuong Quynh Nguyen for her outstanding technical support. GPF was generously provided by Neo Modulus (Suzhou) Medical Sci-Tech Co., Ltd. Zhiwei Tian is grateful for the financial support received from the Association for the Promotion of the Eurasia-Pacific Uninet (APE).

Author contributions
ZT, OA, and XR-F. conceived and designed the study; ZT, ZZ, CB, DT, and OA performed investigation, ZT, ZZ, MAR, and HAS-T collected data; ZT wrote the original draft; ZZ, MAR, CB, DT, HAS-T, OA, and XR-F. reviewed and edited the manuscript; OA and XR-F provided the project administration and supervision; XR-F was responsible for funding acquisition; All authors have read and agreed to the published version of the manuscript.

Funding
This research was funded by the Neo Modulus (Suzhou) Medical Sci-Tech Co., Ltd and the Medical University of Vienna, grant number FA670F0205.

Data availability
The data presented in this study are available on request from the corresponding author.

Declarations

Ethical approval and consent to participate
All procedures performed in studies involving human participants were in accordance with the ethical standards of the institutional and/or national research committee and with the 1964 Helsinki Declaration and its later amendments or comparable ethical standards. The study was approved by the Ethics Committee of the Medical University of Vienna (ethical approval number: 1079/2019, extended in 2025). All participants provided informed consent prior to the study.

Consent to publication
Not applicable.

Competing interests
The authors declare no competing interests.

Author details
[1]Competence Center for Periodontal Research, University Clinic of Dentistry, Medical University of Vienna, Vienna, Austria
[2]Clinical Division of Orthodontics, University Clinic of Dentistry, Medical University of Vienna, Vienna, Austria
[3]Clinical Division of Periodontology, University Clinic of Dentistry, Medical University of Vienna, Vienna, Austria
[4]Core Facility Applied Physics, Laser and CAD/CAM Technology, University Clinic of Dentistry, Medical University of Vienna, Vienna, Austria
[5]Center for Clinical Research, University Clinic of Dentistry, Medical University of Vienna, Vienna, Austria

Received: 15 January 2025 / Accepted: 18 April 2025
Published online: 25 April 2025

References

1. Wang SS, Tang YL, Pang X, Zheng M, Tang YJ, Liang XH. The maintenance of an oral epithelial barrier. Life Sci. 2019;227:129–36. https://doi.org/10.1016/j.lfs.2019.04.029.
2. Moutsopoulos NM, Konkel JE. Tissue-Specific immunity at the oral mucosal barrier. Trends Immunol. 2018;39(4):276–87. https://doi.org/10.1016/j.it.2017.08.005.
3. Bosshardt DD, Lang NP. The junctional epithelium: from health to disease. J Dent Res. 2005;84(1):9–20. https://doi.org/10.1177/154405910508400102.
4. Groeger S, Meyle J. Oral mucosal epithelial cells. Front Immunol. 2019;10:208. https://doi.org/10.3389/fimmu.2019.00208.
5. Polizzi A, Leanza Y, Belmonte A, Grippaudo C, Leonardi R, Isola G. Impact of hyaluronic acid and other Re-Epithelializing agents in periodontal regeneration: A molecular perspective. Int J Mol Sci. 2024;25(22):12347. https://doi.org/10.3390/ijms252212347.
6. Piipponen M, Li D, Landen NX. The immune functions of keratinocytes in skin wound healing. Int J Mol Sci. 2020;21(22):8790. https://doi.org/10.3390/ijms21228790.
7. Schulz S, Angarano M, Fabritius M, Mulhaupt R, Dard M, Obrecht M, Tomakidi P, Steinberg T. Nonwoven-based Gelatin/polycaprolactone membrane proves suitability in a preclinical assessment for treatment of soft tissue defects. Tissue Eng Part A. 2014;20(13–14):1935–47. https://doi.org/10.1089/ten.TEA.2013.0594.
8. Jedrusik N, Steinberg T, Husari A, Volk L, Wang X, Finkenzeller G, Strassburg S, Tomakidi P. Gelatin nonwovens-based epithelial morphogenesis involves a signaling axis comprising EGF-receptor, MAP kinases ERK 1/2, and beta1 integrin. J Biomed Mater Res A. 2019;107(3):663–77. https://doi.org/10.1002/jbm.a.36585.
9. Nagaoka T, Kaburagi Y, Hamaguchi Y, Hasegawa M, Takehara K, Steeber DA, Tedder TF, Sato S. Delayed wound healing in the absence of intercellular adhesion molecule-1 or L-selectin expression. Am J Pathol. 2000;157(1):237–47. https://doi.org/10.1016/S0002-9440(10)64534-8.
10. Nemec M, Behm C, Sedlak M, Nemec-Neuner H, Nguyen PQ, Jonke E, Andrukhov O. Effects of the saliva of patients undergoing orthodontic treatment with invisalign and brackets on human gingival fibroblasts and oral epithelial cells. J Clin Med. 2023;12(23):7440. https://doi.org/10.3390/jcm12237440.
11. Macleod T, Berekmeri A, Bridgewood C, Stacey M, McGonagle D, Wittmann M. The immunological impact of IL-1 family cytokines on the epidermal barrier. Front Immunol. 2021;12:808012. https://doi.org/10.3389/fimmu.2021.808012.
12. Zhou T, Wang N, Xue Y, Ding T, Liu X, Mo X, Sun J. Electrospun tilapia collagen nanofibers accelerating wound healing via inducing keratinocytes proliferation and differentiation. Colloids Surf B Biointerfaces. 2016;143:415–22. https://doi.org/10.1016/j.colsurfb.2016.03.052.
13. Langer R, Vacanti JP. Tissue engineering. Science. 1993;260(5110):920–6. https://doi.org/10.1126/science.8493529.
14. Park J, Park S, Kim JE, Jang KJ, Seonwoo H, Chung JH. Enhanced osteogenic differentiation of periodontal ligament stem cells using a graphene Oxide-Coated Poly(epsilon-caprolactone) scaffold. Polym (Basel). 2021;13(5):797. https://doi.org/10.3390/polym13050797.
15. Thoma DS, Zeltner M, Hilbe M, Hammerle CH, Husler J, Jung RE. Randomized controlled clinical study evaluating effectiveness and safety of a volume-stable collagen matrix compared to autogenous connective tissue grafts for soft tissue augmentation at implant sites. J Clin Periodontol. 2016;43(10):874–85. https://doi.org/10.1111/jcpe.12588.
16. Asparuhova MB, Stahli A, Guldener K, Sculean A. A novel Volume-Stable collagen matrix induces changes in the behavior of primary human oral fibroblasts, periodontal ligament, and endothelial cells. Int J Mol Sci. 2021;22(8):4051. https://doi.org/10.3390/ijms22084051.
17. Zhang S, Huang Y, Yang X, Mei F, Ma Q, Chen G, Ryu S, Deng X. Gelatin nanofibrous membrane fabricated by electrospinning of aqueous gelatin solution for guided tissue regeneration. J Biomed Mater Res A. 2009;90(3):671–9. https://doi.org/10.1002/jbm.a.32136.
18. Xu X, Ren S, Li L, Zhou Y, Peng W, Xu Y. Biodegradable engineered fiber scaffolds fabricated by electrospinning for periodontal tissue regeneration. J Biomater Appl. 2021;36(1):55–75. https://doi.org/10.1177/08853282209522 50.

19. Jedrusik N, Meyen C, Finkenzeller G, Stark GB, Meskath S, Schulz SD, Steinberg T, Eberwein P, Strassburg S, Tomakidi P. Nanofibered Gelatin-Based nonwoven elasticity promotes epithelial histogenesis. Adv Healthc Mater. 2018;7(10):e1700895. https://doi.org/10.1002/adhm.201700895.
20. Chen X, Liu Y, Miao L, Wang Y, Ren S, Yang X, Hu Y, Sun W. Controlled release of Recombinant human cementum protein 1 from electrospun multiphasic scaffold for cementum regeneration. Int J Nanomed. 2016;11:3145–58. https://doi.org/10.2147/IJN.S104324.
21. Shalumon KT, Sowmya S, Sathish D, Chennazhi KP, Nair SV, Jayakumar R. Effect of incorporation of nanoscale bioactive glass and hydroxyapatite in PCL/chitosan nanofibers for bone and periodontal tissue engineering. J Biomed Nanotechnol. 2013;9(3):430–40. https://doi.org/10.1166/jbn.2013.1559.
22. Tian Z, Zhao Z, Rausch MA, Behm C, Shokoohi-Tabrizi HA, Andrukhov O, Rausch-Fan X. In vitro investigation of Gelatin/Polycaprolactone nanofibers in modulating human gingival mesenchymal stromal cells. Mater (Basel). 2023;16(24):7508. https://doi.org/10.3390/ma16247508.
23. Tian Z, Zhao Z, Rausch MA, Behm C, Shokoohi-Tabrizi HA, Andrukhov O, Rausch-Fan X. In vitro investigation of Gelatin/Polycaprolactone nanofibers in modulating human gingival mesenchymal stromal cells. Materials. 2023;16(24). https://doi.org/10.3390/ma16247508.
24. Buskermolen JK, Reijnders CM, Spiekstra SW, Steinberg T, Kleverlaan CJ, Feilzer AJ, Bakker AD, Gibbs S. Development of a Full-Thickness human gingiva equivalent constructed from immortalized keratinocytes and fibroblasts. Tissue Eng Part C Methods. 2016;22(8):781–91. https://doi.org/10.1089/ten.TEC.2016.0066.
25. Kurosawa Y, Yamaguchi H, Uemichi K, Shinozuka K, Kirihara Y, Tsuda H. Butyrate-treatment induces gingival epithelial cell death in a three-dimensional gingival-connective tissue hybrid co-culture system. J Dent Sci. 2023;18(2):893–7. https://doi.org/10.1016/j.jds.2022.08.034.
26. Nemec M, Bartholomaeus HM, Behm MHB, Ali Shokoohi-Tabrizi C, Jonke H, Andrukhov E, Rausch-Fan O. SmartTrack((R)) material. Mater (Basel). 2020;13(23):5311. https://doi.org/10.3390/ma13235311. ((R)). Behaviour of Human Oral Epithelial Cells Grown on Invisalign.
27. Guo B, Tang C, Wang M, Zhao Z, Shokoohi-Tabrizi HA, Shi B, Andrukhov O, Rausch-Fan X. In vitro biocompatibility of biohybrid polymers membrane evaluated in human gingival fibroblasts. J Biomed Mater Res B Appl Biomater. 2020;108(6):2590–8. https://doi.org/10.1002/jbm.b.34591.
28. Rausch MA, Shokoohi-Tabrizi H, Wehner C, Pippenger BE, Wagner RS, Ulm C, Moritz A, Chen J, Andrukhov O. Impact of implant surface material and microscale roughness on the initial attachment and proliferation of primary human gingival fibroblasts. Biology (Basel). 2021;10(5):356. https://doi.org/10.3390/biology10050356.
29. Dieterle MP, Steinberg T, Tomakidi P, Nohava J, Vach K, Schulz SD, Hellwig E, Proksch S. Novel in Situ-Cross-Linked electrospun gelatin/hydroxyapatite nonwoven scaffolds prove suitable for periodontal tissue engineering. Pharmaceutics. 2022;14(6):1286. https://doi.org/10.3390/pharmaceutics14061286.
30. Patil SV, Nanduri LSY. Interaction of Chitin/chitosan with salivary and other epithelial cells-An overview. Int J Biol Macromol. 2017;104(Pt B):1398–406. https://doi.org/10.1016/j.ijbiomac.2017.03.058.
31. Chen X, Bai S, Li B, Liu H, Wu G, Liu S, Zhao Y. Fabrication of gelatin methacrylate/nanohydroxyapatite microgel arrays for periodontal tissue regeneration. Int J Nanomed. 2016;11:4707–18. https://doi.org/10.2147/IJN.S111701.
32. Lakra R, Kiran MS, Korrapati PS. Electrospun gelatin-polyethylenimine blend nanofibrous scaffold for biomedical applications. J Mater Sci Mater Med. 2019;30(12):129. https://doi.org/10.1007/s10856-019-6336-5.
33. Haase I, Evans R, Pofahl R, Watt FM. Regulation of keratinocyte shape, migration and wound epithelialization by IGF-1- and EGF-dependent signalling pathways. J Cell Sci. 2003;116(Pt 15):3227–38. https://doi.org/10.1242/jcs.00610.
34. Rungsiyanont S, Dhanesuan N, Swasdison S, Kasugai S. Evaluation of biomimetic scaffold of gelatin-hydroxyapatite crosslink as a novel scaffold for tissue engineering: biocompatibility evaluation with human PDL fibroblasts, human mesenchymal stromal cells, and primary bone cells. J Biomater Appl. 2012;27(1):47–54. https://doi.org/10.1177/0885328210391920.
35. Kuppan P, Sethuraman S, Krishnan UM. PCL and PCL-gelatin nanofibers as esophageal tissue scaffolds: optimization, characterization and cell-matrix interactions. J Biomed Nanotechnol. 2013;9(9):1540–55. https://doi.org/10.1166/jbn.2013.1653.
36. Eberwein P, Steinberg T, Schulz S, Zimmermann D, Accardi R, Beck D, Reinhard T, Tomakidi P. Expression of keratinocyte biomarkers is governed by environmental biomechanics. Eur J Cell Biol. 2011;90(12):1029–40. https://doi.org/10.1016/j.ejcb.2011.08.005.
37. Steinberg T, Schulz S, Spatz JP, Grabe N, Mussig E, Kohl A, Komposch G, Tomakidi P. Early keratinocyte differentiation on micropillar interfaces. Nano Lett. 2007;7(2):287–94. https://doi.org/10.1021/nl062271z.
38. Gumusderelioglu M, Kaya FB, Beskardes IG. Comparison of epithelial and fibroblastic cell behavior on nano/micro-topographic PCL membranes produced by crystallinity control. J Colloid Interface Sci. 2011;358(2):444–53. https://doi.org/10.1016/j.jcis.2011.03.026.
39. Qiang L, Yang S, Cui YH, He YY. Keratinocyte autophagy enables the activation of keratinocytes and fibroblastsand facilitates wound healing. Autophagy. 2021;17(9):2128–43. https://doi.org/10.1080/15548627.2020.1816342.
40. Fujimura T, Mitani A, Fukuda M, Mogi M, Osawa K, Takahashi S, Aino M, Iwamura Y, Miyajima S, Yamamoto H, et al. Irradiation with a low-level diode laser induces the developmental endothelial locus-1 gene and reduces Pro-inflammatory cytokines in epithelial cells. Lasers Med Sci. 2014;29(3):987–94. https://doi.org/10.1007/s10103-013-1439-6.
41. Zhao Z, Behm C, Rausch MA, Tian Z, Rausch-Fan X, Andrukhov O. Cyclic tensile strain affects the response of human periodontal ligament stromal cells to tumor necrosis factor-alpha. Clin Oral Investig. 2022;26(1):609–22. https://doi.org/10.1007/s00784-021-04039-8.
42. Ren K, Wang Y, Sun T, Yue W, Zhang H. Electrospun PCL/gelatin composite nanofiber structures for effective guided bone regeneration membranes. Mater Sci Eng C Mater Biol Appl. 2017;78:324–32. https://doi.org/10.1016/j.msec.2017.04.084.
43. Tian Z, Zhao Z, Rausch MA, Behm C, Tur D, Shokoohi-Tabrizi HA, Andrukhov O, Rausch-Fan X. Potential of trilayered Gelatin/Polycaprolactone nanofibers for periodontal regeneration: an in vitro study. Int J Mol Sci. 2025;26(2). https://doi.org/10.3390/ijms26020672.
44. Andrukhov O, Huber R, Shi B, Berner S, Rausch-Fan X, Moritz A, Spencer ND, Schedle A. Proliferation, behavior, and differentiation of osteoblasts on surfaces of different microroughness. Dent Mater. 2016;32(11):1374–84. https://doi.org/10.1016/j.dental.2016.08.217.
45. Jiang W, Li L, Zhang D, Huang S, Jing Z, Wu Y, Zhao Z, Zhao L, Zhou S. Incorporation of aligned PCL-PEG nanofibers into porous Chitosan scaffolds improved the orientation of collagen fibers in regenerated periodontium. Acta Biomater. 2015;25:240–52. https://doi.org/10.1016/j.actbio.2015.07.023.
46. McNamara LE, Burchmore R, Riehle MO, Herzyk P, Biggs MJ, Wilkinson CD, Curtis AS, Dalby MJ. The role of microtopography in cellular mechanotransduction. Biomaterials. 2012;33(10):2835–47. https://doi.org/10.1016/j.biomaterials.2011.11.047.
47. Gauthier R, Attik N, Chevalier C, Salles V, Grosgogeat B, Gritsch K, Trunfio-Sfarghiu AM. 3D electrospun Polycaprolactone scaffolds to assess human periodontal ligament cells Mechanobiological behaviour. Biomimetics (Basel). 2023;8(1). https://doi.org/10.3390/biomimetics8010108.
48. Imber JC, Roccuzzo A, Stahli A, Saulacic N, Deschner J, Sculean A, Bosshardt DD. Immunohistochemical evaluation of periodontal regeneration using a porous collagen scaffold. Int J Mol Sci. 2021;22(20). https://doi.org/10.3390/ijms222010915.
49. Thoma DS, Gasser TJW, Hammerle CHF, Strauss FJ, Jung RE. Soft tissue augmentation with a volume-stable collagen matrix or an autogenous connective tissue graft at implant sites: Five-year results of a randomized controlled trial post implant loading. J Periodontol. 2023;94(2):230–43. https://doi.org/10.1002/JPER.22-0226.
50. Sakai Y, Nemoto E, Kanaya S, Shimonishi M, Shimauchi H. Calcium phosphate particles induce interleukin-8 expression in a human gingival epithelial cell line via the nuclear factor-kappaB signaling pathway. J Periodontol. 2014;85(10):1464–73. https://doi.org/10.1902/jop.2014.130709.
51. Xiao L, Okamura H, Kumazawa Y. Three-dimensional inflammatory human tissue equivalents of gingiva. J Vis Exp: JoVE. 2018(134). https://doi.org/10.3791/57157
52. Usui M, Sato T, Yamamoto G, Okamatsu Y, Hanatani T, Moritani Y, Sano K, Yamamoto M, Nakashima K. Gingival epithelial cells support osteoclastogenesis by producing receptor activator of nuclear factor kappa B ligand via protein kinase A signaling. J Periodontal Res. 2016;51(4):462–70. https://doi.org/10.1111/jre.12323.
53. Fernandez-Gutierrez MM, Roosjen PPJ, Ultee E, Agelink M, Vervoort JJM, Keijser B, Wells JM, Kleerebezem M. Streptococcus salivarius MS-oral-D6 promotes gingival re-epithelialization in vitro through a secreted Serine protease. Sci Rep. 2017;7(1):11100. https://doi.org/10.1038/s41598-017-11446-z.
54. Boloori E, Schoenmaker T, Kleverlaan CJ, Loos BG, de Vries TJ. Gingival epithelium attachment to well- or partially cured resin composites. Eur Cell Mater. 2020;40:259–75. https://doi.org/10.22203/eCM.v040a16.

55. Enaka M, Nakanishi M, Muragaki Y. The Gain-of-Function mutation p53R248W suppresses cell proliferation and invasion of oral squamous cell carcinoma through the Down-Regulation of keratin 17. Am J Pathol. 2021;191(3):555–66. https://doi.org/10.1016/j.ajpath.2020.11.011.

Publisher's note